Tenth USA/Europe Air Traffic Management Research and Development Seminar (ATM2013)

Applying Flight-deck Interval Management based Continuous Descent Operation for Arrival Air Traffic to Tokyo International Airport

Eri Itoh and Kazuhiko Uejima
Air Traffic Management department,
Electronic Navigation Research Institute (ENRI)
Chofu, Tokyo, Japan
{eri, k-uejima}@enri.go.jp

***Abstract*—Aiming to realize Continuous Descent Operation (CDO) in high-density air traffic, Flight-deck Interval Management (FIM) is seen as one of the promising applications in the Aircraft Surveillance Applications System (ASAS). In the FIM application, an aircraft's arrival time at an airport is estimated while it is in flight, and its airspeed is controlled to achieve an assigned time spacing between its immediately preceding aircraft at the runway threshold. In order to evaluate the performance of the FIM application, this paper simulates CDO based on the FIM application for arrivals at Tokyo International Airport. A medium-fidelity aircraft model, which includes Vertical/Lateral NaVigation (VNAV/LNAV) autopilot modes, an engine system, and a Total Energy Control System (TECS), is implemented in a fast-time simulation. Potential CDO arrival routes at Tokyo International Airport are proposed. The simulation results evaluate the accuracy of FIM-based time spacing and fuel consumption. Wind estimation errors are considered in this paper.**

Keywords- Flight-deck Interval Management (FIM); Continuous Descent Operation (CDO); Aircraft Surveillance Applications System (ASAS); Time-spacing; fuel consumption; tragectory management

I. INTRODUCTION

Continuous Descent Operation (CDO) [1-3], in which arriving aircraft descend from cruise to an airport at near-idle thrust, is expected to realize even better energy saving arrivals in the future. Currently, continuous descent is doable only in low-density traffic to avoiding conflicts between aircraft. In order to apply CDO in high-density operations, more accurate time spacing between arriving aircraft must be achieved. One proposal to realize accurate time spacing in CDO is Flight-deck Interval Management (FIM) [4]. FIM is one of the airborne based time spacing applications in the Aircraft Surveillance Applications System (ASAS), previously known as the Airborne Separation Assurance/Assistance System [5, 6].

ASAS covers a range of applications to allow for a gradual shifting of tasks from Air Traffic Controllers (ATCo) to pilots by using flight information on surrounding air traffic received via the Airborne Dependent Surveillance–Broadcast (ADS-B) data link. One ASAS application of great interest is Interval Management (IM), previously known as the Sequencing and Merging (S&M) application. IM is expected to achieve an assigned time spacing between a leading aircraft and another following it in trail by speed control. Our earlier study developed an initial mathematical model of airborne time spacing by speed control using ADS-B surveillance information which we call "ASAS speed control". Its performance and safety were evaluated by numerical simulation [7-12], and the results showed that ASAS speed control is feasible and effective for CDO. A more advanced ASAS speed control law has been studied as the FIM application, which is the airborne counterpart to IM [4, 13-15]. In the FIM speed control law, the arrival time of the leading aircraft is first estimated following the planned flight trajectory, then a target speed for an aircraft following it is calculated to achieve an assigned time spacing from the leading aircraft at the runway threshold using its estimated time of arrival. Our next challenge is to clarify the effectiveness of the FIM application by simulating this combination of trajectory prediction and the speed control law for arrivals to Tokyo International Airport.

Tokyo International Airport is one of the world's busiest airports by passenger traffic. A new terminal building for international flights and a new runway opened in 2010 aiming to increase its capacity to 410,000 movements per year. Currently, continuous descent is realized only when the traffic is not congested (for example, between midnight and 6 am), but not during busy times, when aircraft land every two minutes. This is for safety reasons since a continuous descent sometimes demands ground-based airspeed prediction accuracy which is difficult to achieve, so extra separation margins are given between arrival aircraft to achieve separation reliably. This is the reason that ensuring accurate time spacing is needed to realize continuous descents in high-density operations while maintaining or increasing the arrival rate. This paper applies FIM operation to CDO and discusses the performance of time spacing and the amount of fuel burn reduction. Designs of arrival routes to realize CDO at Tokyo International Airport are also proposed.

This paper is organized as follows. Firstly, current arrival operations at Tokyo International Airport are explained, and arrival routes for realizing CDO are proposed. Secondly, FIM-based CDO is implemented in a fast-time simulation with a

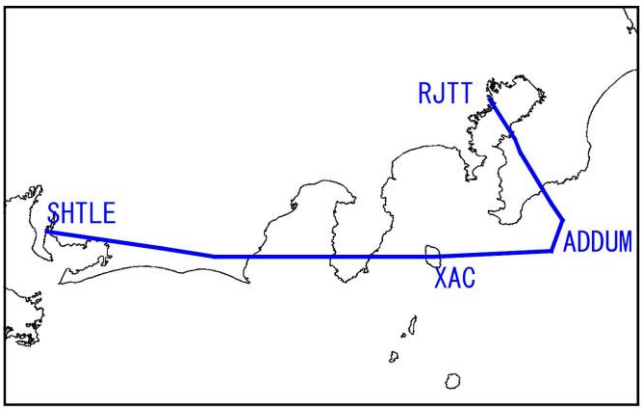

Figure 1. Current RNAV routes to RW34L (Lateral)

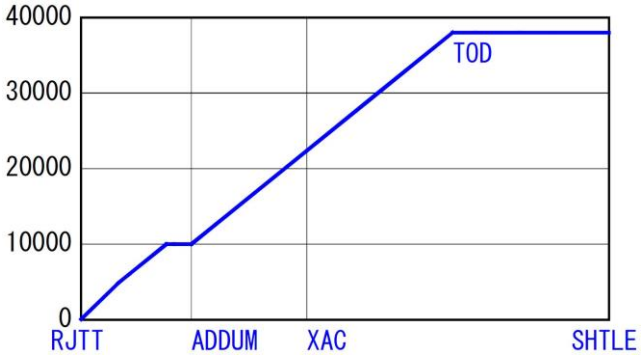

Figure 2. Current RNAV routes to RW34L (Vertical)

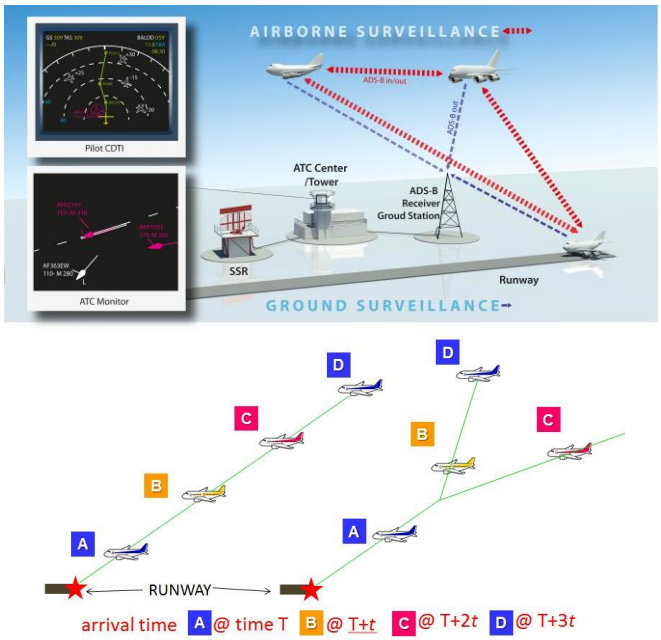

Figure 3. Overview of ASAS and FIM application: *The above figure shows a concept of ASAS. Figure below shows FIM operation. ATCo decides a sequence of arrivals and time interval t at a runway threshold between its leading aircraft. Airspeed is controlled in the air following ATCo's instruction. It is applicable for a traffic which merges as shown in the right figure.*

medium-fidelity aircraft model [16] which includes Vertical/Lateral NaVigation (VNAV/LNAV) autopilot modes, an engine system, and a Total Energy Control System (TECS). Monte Carlo simulations are conducted to evaluate the time spacing performance. Fuel consumption is calculated using engine model parameters and compared with actual data taken from Boeing 777-200 aircraft. Simulation results are discussed to evaluate the performance of the FIM-based CDO applied to Tokyo International Airport arrivals. Lastly, future works are summarized in the concluding remarks.

II. Energy Saving Arrivals

A. Current Arrival Operations at Tokyo International Airport

Tokyo International Airport is open 24 hours, and has four runways to allow 410,000 movements per year. This paper focuses on domestic flights from west and south Japan arriving on RunWay 34L (RW34L), which is the most frequently used runway during the winter season. In high-density operations, an aircraft lands on RW34L every two minutes.

Figures 1 and 2 show one of the currently used aRea NAVigation (RNAV) routes to RW34L. Aircraft on different airways are merged at a waypoint named DIIVA, and cross a terminal gate at ADDUM. Since an altitude restriction is imposed to cross ADDUM at below 10,000 feet, this does not allow a continuous descent on a 2.5-degree path angle (our research employs a 2.5-degree path angle for continuous descent to the airport) to be drawn from ADDUM to capture the Instrument Landing System (ILS) glide slope (3.0-degree path angle) as shown in Fig. 2. Avoiding level flight after passing ADDUM requires removal of the altitude restriction or flying "shortcut" routes to RW34L.

B. Flight-deck Interval Management (FIM)

To achieve accurate time spacing in CDO at Tokyo International Airport, we apply the Flight-deck Interval Management (FIM) application [4] of the Aircraft Surveillance Applications System (ASAS) [5,6]. ASAS covers a range of applications which use the ADS-B data link to allow for a gradual shift of tasks from ATCos to pilots. It consists of an integrated air-to-air and air-to-ground system which enables aircraft to obtain information on surrounding air traffic via ADS-B surveillance. It shifts part of the ATCo's task to pilots and allows pilots to maintain airborne separation by visualizing traffic information on a cockpit display. Figure 3 shows the basic concept of ASAS and the FIM application.

In the FIM application, the ATCo decides the arrival sequence and desired time intervals at the runway threshold. The ATCo gives instructions to each aircraft, designating a leading aircraft to follow and the required time interval to the leading aircraft at the runway threshold. Pilots then "capture" the leading aircraft via ADS-B information on the cockpit monitor, and airspeed is controlled to achieve the assigned time interval. The ATCo remains responsible for aircraft separation during FIM operations.

The FIM application's speed control law, which gives a target airspeed to fly to achieve the assigned time interval, has been developed as the ASTAR algorithm by NASA's Langley Research Center [13-15]. It consists of three main

components: an air route design, a trajectory generator, and a speed controller.

- Air route design
  An air route is designed as a sequence of waypoints which aircraft pass through flying to the runway threshold. Latitude, longitude, crossing altitude/glide path angle, crossing airspeed, ratio of airspeed, and wind data are defined at each waypoint.
- Trajectory Generator [14, 15]
  A four-dimensional (4D) aircraft trajectory to follow a designed air route, including lateral, vertical, and speed profile, is generated. Distance to the runway threshold (Distance To Go: DTG) and estimated time to the runway threshold (Time To Go: TTG) are calculated from the current aircraft state and the 4D trajectory.
- Speed Controller [15]
  Based on the DTG and TTG of the leading aircraft and the aircraft itself (the "ownship"), the ownship's speed is controlled in order to achieve the assigned time interval at the runway threshold. A notch filter and gain settings in the speed controller determine when the speed control starts depending on the DTG of the ownship. The maximum and minimum speeds demanded by the controller are limited to within ±10% of the airspeed in the speed profile in the generated 4D trajectory. The VNAV PATH autopilot mode is used for vertical flight profile control.

The latest version of ASTAR, version 11, was released in 2012. The input to ASTAR is the necessary waypoint information to define air routes, and the output is a speed command. Our preliminary study implemented the ASTAR algorithm with a low-fidelity point-mass aircraft model in a fast-time simulation environment, and estimated the behavior of the speed control given by ASTAR for Tokyo International Airport arrivals. This simulation study indicated the following two points: (1) FIM defines a single air route for all aircraft conducting FIM operations flying through the same set of waypoints. It is therefore needed to confirm that the designed air routes are suitable for all applicable aircraft types. For example, the achievable ratio of airspeed change and combinations of airspeed and glide slope angle vary with aircraft type (e.g. the B777-200 and B737-800 have their own optimal profiles). Medium-fidelity aircraft models are therefore required for the further study of FIM operations, particularly during the descent phase. (2) The performance of the achieved time spacing depends on the designed air routes. Moreover, notch filters parameter and gain values in the speed controller determine when and how speed control starts on routes, and these values are also assumed to affect FIM performance.

From the above preliminary study findings, this paper describes a follow-on fast-time simulation study based on a modeling approach and evaluates the performance of FIM-based CDO at Tokyo International Airport from the perspectives of time spacing accuracy and fuel consumption. Simulation assumptions, including proposed air route designs, are described in the next section.

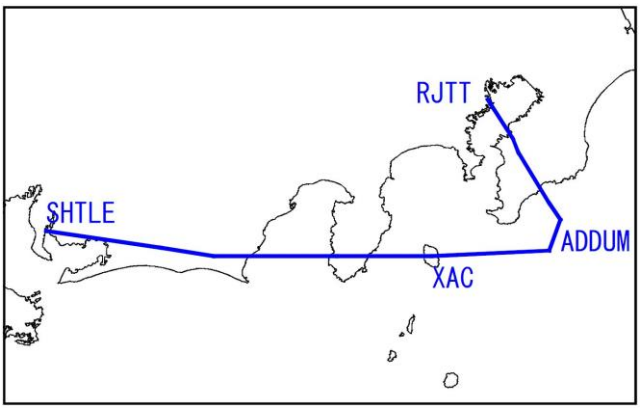

Figure 4 Route A lateral path: *no altitude restriction at ADDUM*

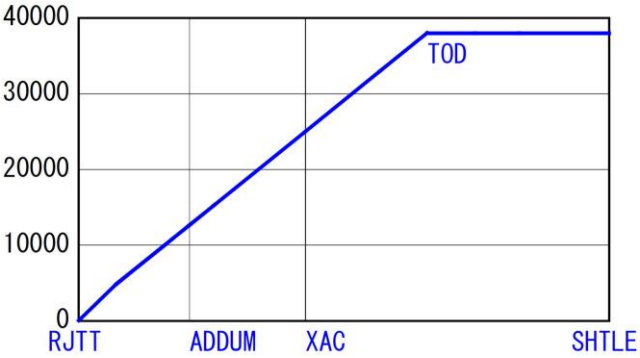

Figure 5 Route A vertical path: *no altitude restriction at ADDUM*

III. Simulation Assumptions

A. Air route design for CDO to Tokyo International Airport

In order to realize CDO for Tokyo International Airport arrival traffic, this paper proposes the following three air routes designs. These designs do not take into account interactions with other arrival/departure flight routes.

1) No altitude restriction at ADDUM

Since the altitude restriction at the ADDUM terminal gate prevents continuous descent to RW34L as shown in Fig. 2, one possibility to realize CDO is to remove this restriction. Figures 4 and 5 show the lateral and vertical paths of the designed air routes. As shown in Fig. 5, the crossing altitude is established by drawing 2.5-degree glide slope from the ILS approach. We call this route "Route A" below.

2) Cross OSHIMA(XAC) direct to KAIHO

Another possibility to realize CDO is to select a shortcut from the OSHIMA (XAC) waypoint directly to the KAIHO waypoint. The lateral and vertical paths from SHTLE, which is 177.46 nm from the threshold of RW34L following this "short cut" route, are shown in Figs. 6 and 7. Figure 7 shows that a 2.5-degree glide slope is drawn from the ILS approach.

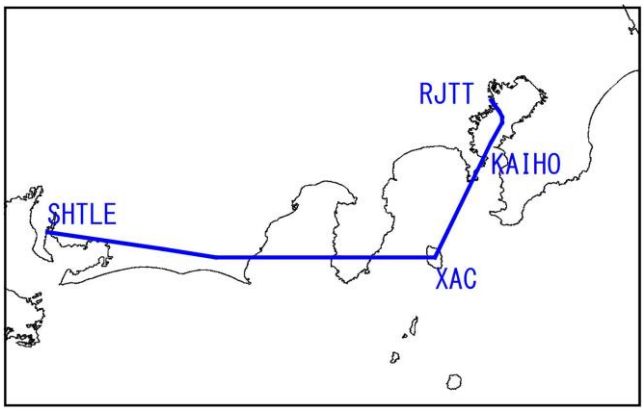

Figure 6 Route K/S lateral path: *Cross OSHIMA (XAC) direct to KAIHO from SHTLE*

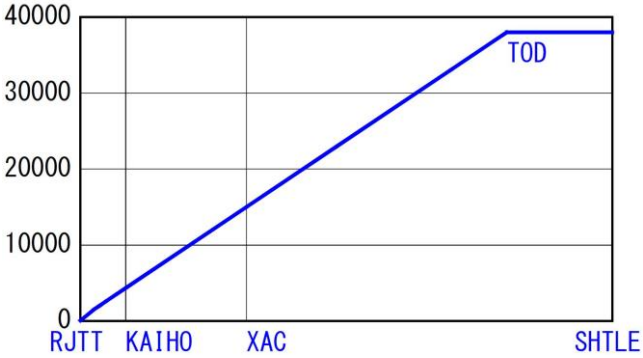

Figure 7 Route K/S vertical path: *Cross OSHIMA (XAC) direct to KAIHO from SHTLE*

Comparing Figs. 4 and 6, this route gives a shortcut from SHTLE while reducing noise impact to urban areas by passing above Tokyo bay. According to an airline pilot, it is one of the most desirable shortcuts to Tokyo International Airport. We call this route "Route K/S".

3) Merge at OSHIMA(XAC) direct to KAIHO

The third route includes merging of a northern arrival route from SHTLE and a southern arrival route from FLUTE at OSHIMA (XAC). Figure 8 shows the lateral path, and Fig. 9 shows the vertical path of the southern arrival from FLUTE, which is 178.182 nm along the route from RW34L. The vertical path of the northern arrival from SHTLE is shown in Fig. 7. This route is a shortcut to RW34L crossing KAIHO, and includes the merging of aircraft conducting CDO. As shown in Figs. 7 and 9, a 2.5-degree continuous descent glide slope is drawn from the ILS approach. We call the southern route "Route K/F".

B. Assumptions

1) Functional characteristics

Aircraft are assumed to be equipped with standard navigation and communication systems, plus ADS-B and ASAS. A simplified equipage composition is SSR transponder, ADS-B transmitter/receiver, ASAS spacing director, ASAS airside avionics, Flight Management System (FMS), Inertial Navigation System (INS), and Global Navigation Satellite

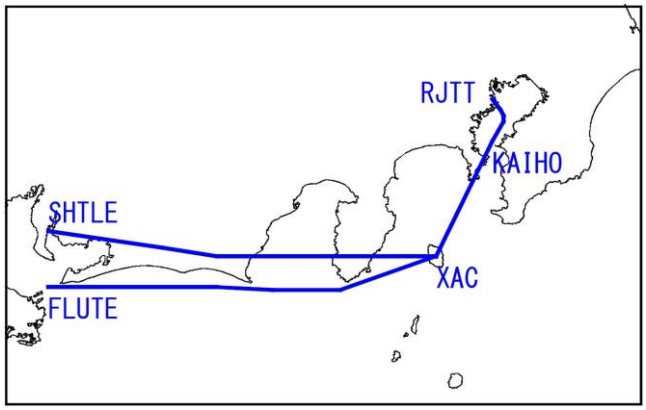

Figure 8 Route K/F lateral path: *Merge at OSHIMA (XAC) direct to KAIHO from SHTLE/FLUTE*

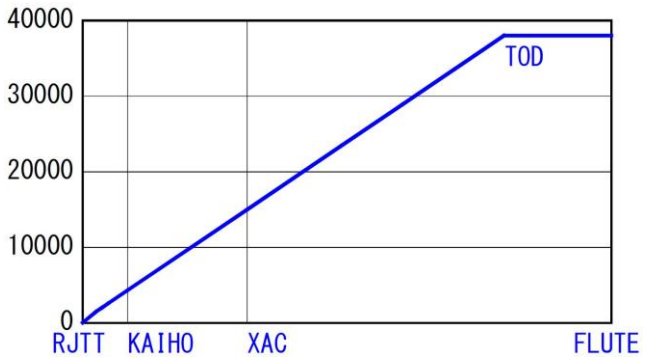

Figure 9 Route K/F vertical path: *Cross OSHIMA (XAC) direct to KAIHO from FLUTE*

System (GNSS). The ground system has standard terminal area and en-route surveillance systems, plus the ASAS ground counterpart.

This paper employs two types of aircraft model: B777-200 and B737-800. For running a fast-time simulation, we built medium-fidelity mathematical models of the aircraft which implement VNAV and LNAV autopilot modes, an engine system, a TECS, and the combination of trajectory prediction and speed control algorithms in the FIM application. To handle the complexity of the modeling, we make use of an extended Petri net formalism, Stochastically and Dynamically Coloured Petri Net (SDCPN) [17-20], which represents complex systems including stochastic behaviors and dynamic processes. These modeling works are summarized in [21].

2) Operational goals

We consider the three RNAV routes designed above (Figs. 4-9). Aircraft descend from 38,000 feet to the Final Approach Fix (FAF) at a 2.5-degree path angle, and then follow the ILS approach 3.0-degree glide slope. Speed profiles are given so as to remain within the flight envelope and to observe the ATC maximum speed restriction of 250 knots below 10,000 ft.

The FIM execution procedure comprises the following three phases: initiation, execution, and termination. In the initiation phase, an ATCo identifies a pair of leading and following

aircraft and assigns a desired time spacing. The ATCo instructs the aircraft to follow the leading aircraft and to achieve the time spacing at the runway threshold if the pilot can identify the leading aircraft via ADS-B surveillance. In the execution phase, the pilot executes FIM to comply with the ATCo instructions. Speed is controlled within ±10 % of the speed profile to achieve the assigned time spacing. Lastly, the FIM operation is terminated at the threshold of RW34L in this study. The execution points are at SHTLE on the northern route and at FLUTE on the southern route. The ATCo decides the arrival sequence and time-spacing intervals 10–15 minutes before FIM operations are executed at SHTLE and FLUTE. An aircraft executing FIM operations (FIM aircraft) identifies the leading aircraft and completes all preparations before crossing the execution point.

This paper considers three pairs of aircraft trailing, a total of four aircraft, in a string. According to an experienced ATCo working at Tokyo International Airport, four is the maximum number of aircraft that can be handled in a string considering cases when ATCos must take over from FIM operation to handle irregularities at Tokyo International Airport, for example closure of RW34L. Crossing aircraft type with air routes gives five cases as shown in Table 1.

TABLE I. AIRCRAFT TYPES AND AIR ROUTES IN ONE STRING (3 PAIRS OF LEADING AND FOLLOWING AIRCRAFT)

Case	Aircraft type (Route name)			
	1st aircraft	2nd aircraft	3rd aircraft	4th aircraft
A	B777-200 (Route A)	B777-200 (Route A)	B777-200 (Route A)	B777-200 (Route A)
B	B777-200 (Route A)	B737-800 (Route A)	B737-800 (Route A)	B777-200 (Route A)
C	B777-200 (Route K/S)	B777-200 (Route K/S)	B777-200 (Route K/S)	B777-200 (Route K/S)
D	B777-200 (Route K/S)	B777-200 (Route K/F)	B777-200 (Route K/S)	B777-200 (Route K/F)
E	B777-200 (Route K/S)	B737-800 (Route K/F)	B737-800 (Route K/S)	B777-200 (Route K/F)

For simplicity, we assume a typical winter seasonal west wind of 100 knots at 40,000 ft decreasing linearly with altitude to 20 knots at RW34L. Wind estimation error is assumed to be 10 knots: actual velocity of the west wind is 10 knots stronger than the estimate during flight. The flap and gear extension schedule depends on aircraft type and airline policies, but we set the following in the aircraft model based on pilot comments: flaps start extending when airspeed reaches 210 knots and take 60 seconds to travel to the landing flap setting. The landing gear is lowered at 1,500 ft altitude.

This paper assumes that once FIM is initiated by the pilot, the ASTAR commanded speed is automatically input to the automatic flight control and autothrottle systems, with no pilot intervention. All cases employ the same parameter values in the speed controller.

In the Monte Carlo simulations, the initial time spacing intervals t_e at the FIM execution waypoints (SHTLE and FLUTE) are given by a uniform density f_U as shown in Equations (1) and (2). In this study, we set the minimum time spacing value as $t_{min} = 105$ (seconds) and the maximum time-spacing value as $t_{max} = 135$ (seconds) considering a ± 15 second deviation from a standard two-minute landing interval, which is the target time spacing at the runway threshold.

Monte Carlo simulations were run 100 times for each case in Table 1. The performances in terms of achieved time spacing and fuel consumption based on the simulation results are examined in the next section.

$$t_e \leftarrow f_U(x;\quad t_{min},\quad t_{max}) \tag{1}$$

$$f_U(x;\quad t_{min},\quad t_{max}) = \begin{cases} \dfrac{1}{t_{max} - t_{min}} & if \quad t_{min} \le x \le t_{max} \\ 0 & else \end{cases} \tag{2}$$

IV. SIMULATION RESULTS

A. Time-spacing performance

1) Route A: No restriction at terminal gate ADDUM

Firstly, we discuss the level of accuracy of time spacing which FIM-based CDO realizes at the runway threshold when arrivals follow Route A (see Figs. 4 and 5), which removes the current altitude restriction at terminal gate ADDUM.

Figures 10–15 show distribution histograms comparing the initial time spacing at the FIM execution waypoint with the achieved time spacing at the runway threshold of each aircraft pair. Figures 10, 11, and 12 show the performances of aircraft for Case A: Fig. 10 shows the time spacing performance achieved by applying FIM speed control during CDO between the first and second aircraft (the first pair in the string), Fig. 11 shows that of the second and third aircraft (the second pair in the string), and Fig. 12 shows that of the third and fourth aircraft (the third pair in the string). Figures 13, 14, and 15 show the performance of aircraft for Case B: Fig. 13 shows the time spacing performance achieved by applying FIM speed control during CDO between the first and second aircraft, Fig. 14 shows that of the second and third aircraft, and Fig. 15 shows that of the third and fourth aircraft. The *x*-axis shows time spacings between the aircraft (seconds), and the *y*-axis shows relative frequency in the Monte Carlo simulation runs (%). In these three figures, the "start" bar shows the distribution of time spacings at the FIM execution waypoint SHTLE (see Figs. 4 and 5) given by a uniform density as shown in Eqs. (1) and (2). The "goal" bar shows the distribution of achieved time spacings at the threshold of RW34L applying FIM speed control during CDO operations. The assigned time spacing value is given as 120 seconds, which is the target value of time spacing to achieve with the leading aircraft at the runway threshold.

Comparing the "start" and "goal" bars in Figs. 10, 11, and 12, the simulation results show that FIM speed control works to reduce the variation of initial time spacing at the FIM execution waypoint SHTLE. Figures 10, 11, and 12 show that the average time spacings at RW34L are 125.400, 125.225, and 124.257 seconds, and their variances are 0.0, 0.005, and 0.173, respectively. The achieved time spacings at the runway

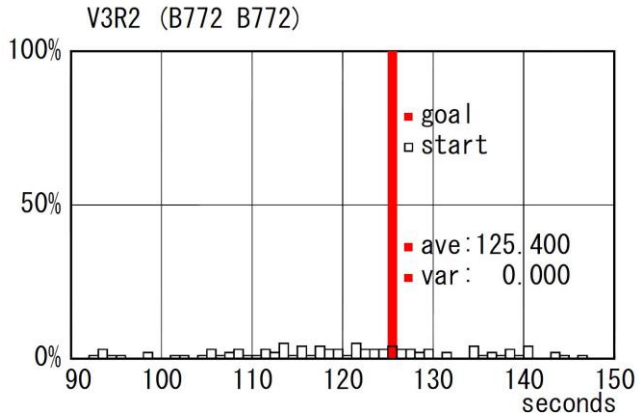

Figure 10 Performance of time spacing between 1st and 2nd aircraft (Case A)

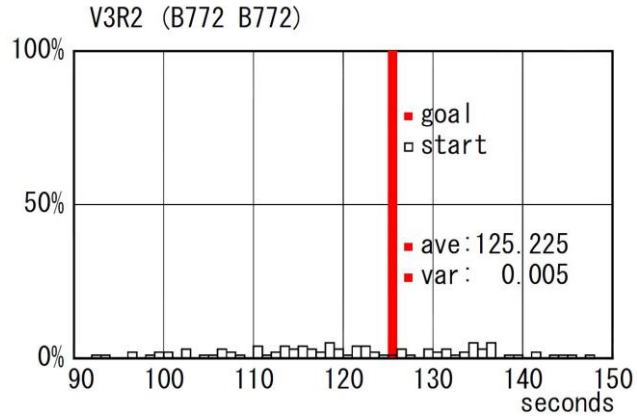

Figure 11 Performance of time spacing between 2nd and 3rd aircraft (Case A)

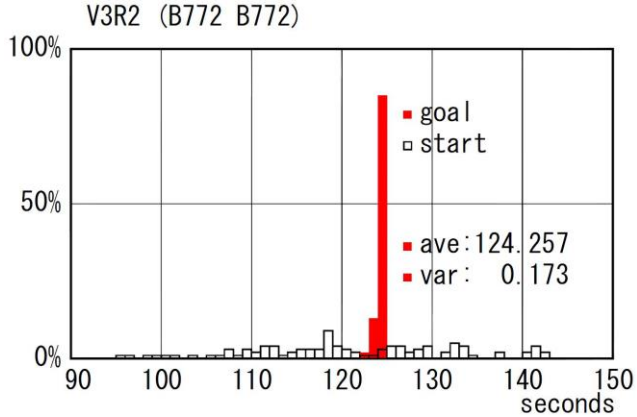

Figure 12 Performance of time spacing between 3rd and 4th aircraft (Case A)

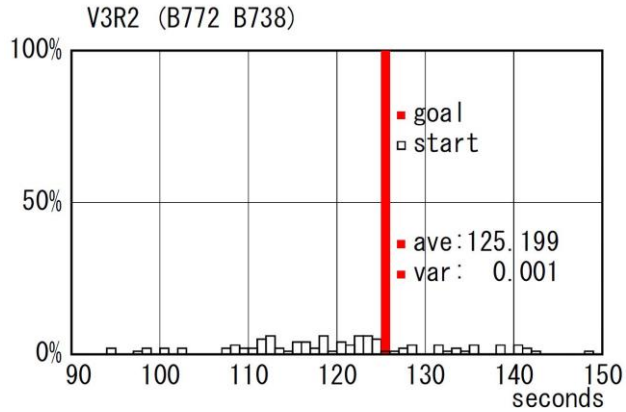

Figure 13 Performance of time spacing between 1st and 2nd aircraft (Case B)

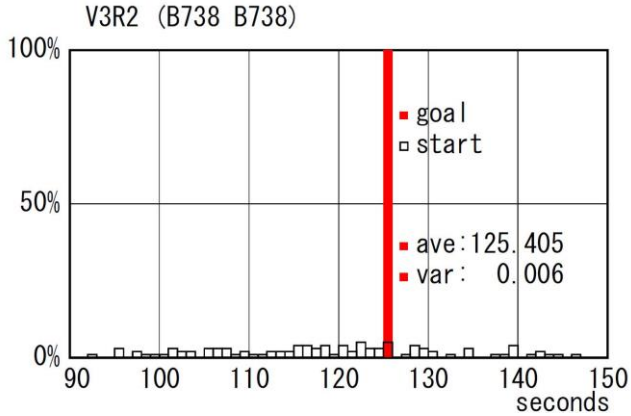

Figure 14 Performance of time spacing between 2nd and 3rd aircraft (Case B)

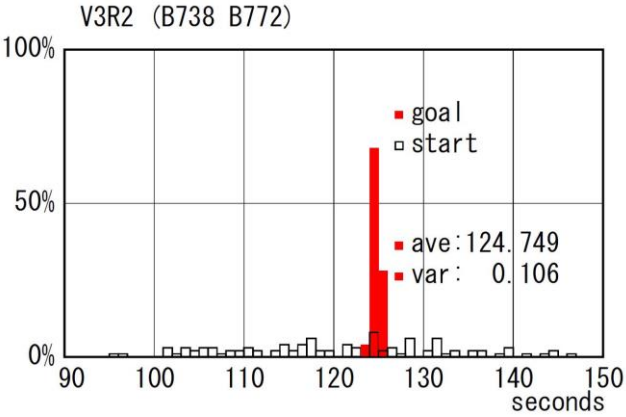

Figure 15 Performance of time spacing between 3rd and 4th aircraft (Case B)

threshold show good convergence, demonstrating that FIM-based CDO can perform to reduce initial time-spacing errors. Since this paper assumed 10 knots errors between velocity of wind and its estimates, it is considered that the average time-spacing at the runway threshold delayed around 5 seconds from the assigned time-spacing of 120 seconds. It is because the arrival time at RW34L was estimated using the estimated wind velocities which was 10 knots smaller than the real velocities of the west wind.

Figures 13, 14, and 15 show the time spacing performance when different aircraft types are combined in a string in Case B: the first aircraft in the string is a B777-200, the second and third are B737-800s, and the fourth is a B777-200. Figures 13, 14, and 15 show that the average time spacings at RW34L are 125.199, 125.405, and 124.749 seconds, and their variances are 0.001, 0.006, and 0.106, respectively. Comparing Figs. 10–12 with 13–15 indicates that the performance of time spacing did not show any dependency on the aircraft types under the simulation assumptions.

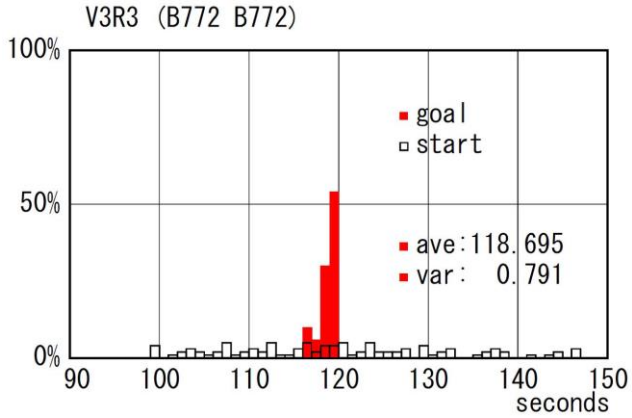

Figure 16 Performance of time spacing between 1st and 2nd aircraft (Case C)

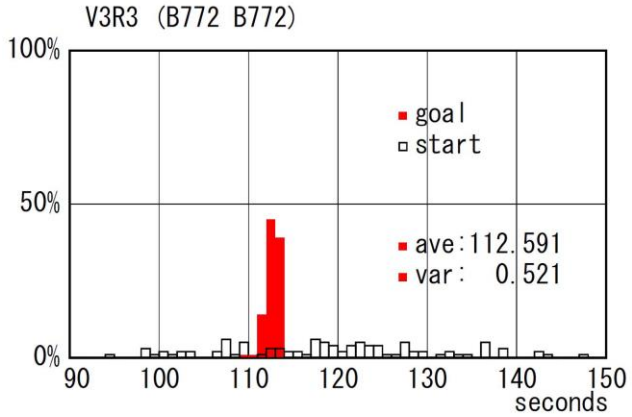

Figure 17 Performance of time spacing between 2nd and 3rd aircraft (Case C)

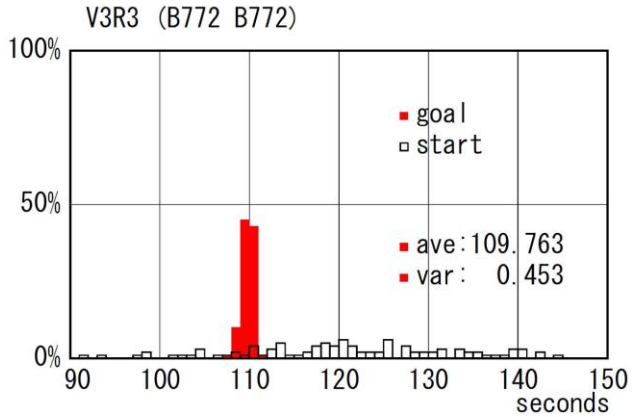

Figure 18 Performance of time spacing between 3rd and 4th aircraft (Case C)

2) Route K/S and Route K/F: OSHIMA(XAC) direct to KAIHO

Secondly, FIM-based CDO was applied to the shortcut routes from OSHIMA (XAC) to RW34L by crossing KAIHO (Route K/S and K/S) shown in Figs. 6–9.

Comparing the "start" and "goal" bars in Figs. 16, 17, and 18, the simulation results show that FIM speed control works to reduce the variation of initial time spacing in Case C. Figures 16, 17, and 18 show that the average time spacings at RW34L are 118.695, 112.591, and 109.763 seconds, and their variances are 0.791, 0.521, and 0.453, respectively. Errors between the average time spacings and the assigned 120-second interval tend to grow in the latter pairs of aircraft under the given simulation assumptions.

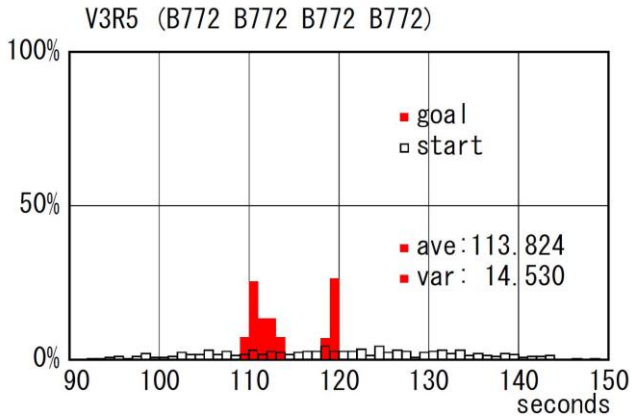

Figure 19 Performance of time spacing: Case D

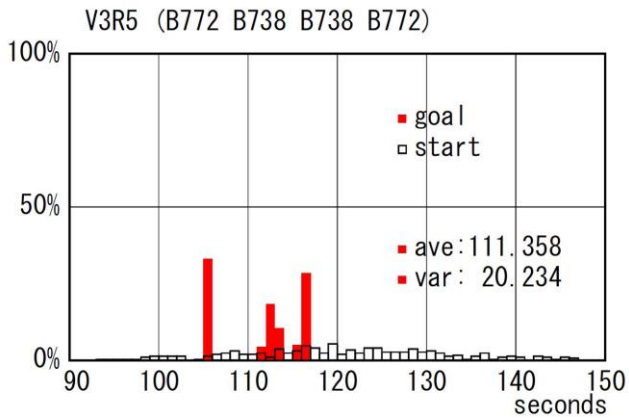

Figure 20 Performance of time spacing: Case E

Comparing Figs. 10–12 with 16–18 indicates that the time spacing performance depends on the air route design even when the aircraft in a string are all of the same type under the simulation assumptions in this paper. One of the reasons considered is the effect of wind estimation errors: the actual west wind was 10 knots stronger than its estimate in the simulation. The west wind was a head wind after passing ADDUM in Case A as shown in Fig. 4. On the other hand, the west wind works as a tail wind while crossing Tokyo bay in Case C as shown in Fig. 6. These results indicate that the wind estimation is one of the key issues to determine the performance of time-spacing in FIM-based CDO.

Figure 19 shows the performance of time spacing in Case D for all four aircraft in the string. All traffic consists of B777-200 types. Figure 20 show the performance of time spacing in Case E for all four aircraft in the string. Furthermore, the traffic consists of a mixture of B777-200 and B737-800 types. The string contains air traffic arriving on different airways merged at OSHIMA (XAC), as shown in Fig. 8 both in Case D and Case E.

Figure 19 shows that the average time spacing at RW34L is 113.824 seconds, and the variance is 14.530. Figure 20 shows that the average time spacing at RW34L is 111.358 seconds, and the variance is 20.234. Comparing Figs. 19 with 20 indicates that the performance of time spacing depends on aircraft type: B737-800s arrive at the runway threshold earlier than B777-200s when B777-200 flies before B737-800 in a string. One reason was found that the VNAV PATH mode was selected in the operational assumptions in the FIM operation. Since VNAV PATH mode controlled elevator angle to follow the vertical path after the B737-800 reached the minimum thrust, airspeed was not decelerated by elevator control. However in this case, it is doable to decelerate airspeed by using speed brake according to pilot's comments. One of the other options is to adjust the value of notch filter gains in the speed controller in order not to control the airspeed aggressively in the early stage after the FIM operation is executed.

B. Fuel Consumption

1) B777-200 fuel consumption from Top Of Descent (TOD)

Next, we discuss the fuel consumption of B777-200 aircraft carrying out CDO applying FIM. Figures 21, 22, 23 and 24 show fuel consumption distribution histograms depending on the aircraft sequence. Since 100 Monte Carlo simulations were run for each case, these figures show the fuel consumption distributions of 100 data points: the *x*-axis is the total fuel consumed from TOD to the runway threshold (lb), and the *y*-axis shows the relative frequency (%). Figures 21, 22, 23, and 24 correspond to the first, second, third, and fourth aircraft, respectively. As shown in these figures, the average fuel consumptions are 2607.232 lb, 2635.471 lb, 2641.324 lb, and 2613.075 lb for the first, second, third, and fourth aircraft, respectively. As shown in Fig. 21, since the first aircraft follows the speed profile defined by the trajectory generator, the value of variance becomes zero. The variance of fuel consumption grows in the successive aircraft: 1803.593, 1816.480, and 3691.272 for the second, third, and fourth aircraft respectively. Since time spacing in the FIM-based CDO is controlled by airspeed, the variance grows in successive aircraft due to engine thrust control. In order not to propagate initial time spacing errors to following aircraft in the string and to minimize errors with the assigned time spacing, thrust changes are required with increasing frequency the further an aircraft is towards the rear of the string.

2) Comparison of simulated B777-200 fuel consumption with actual data

To validate the simulated fuel consumptions in Figs. 21, 22, 23, and 24, simulation results are compared with actual data. We selected actual data from B777-200 arrivals at airports in Japan which achieved ideal descent profiles [22]. These include fuel consumption data of aircraft, which do not only arriving at Tokyo International Airport, but also arriving at the other airport (where frequency of arrivals is lower than that of Tokyo International Airport) in Japan. Figure 25 compares the fuel consumption and required time from TOD from actual

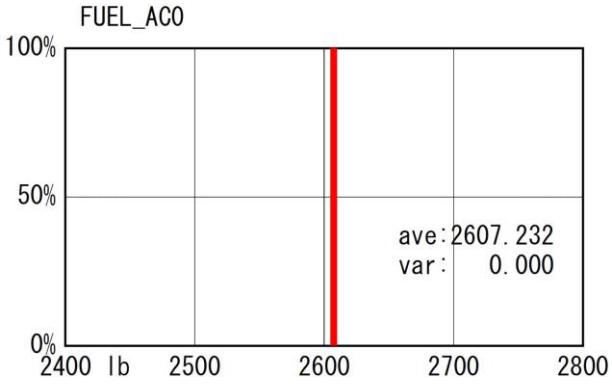

Figure 21 Fuel consumption of B777-200: 1st aircraft

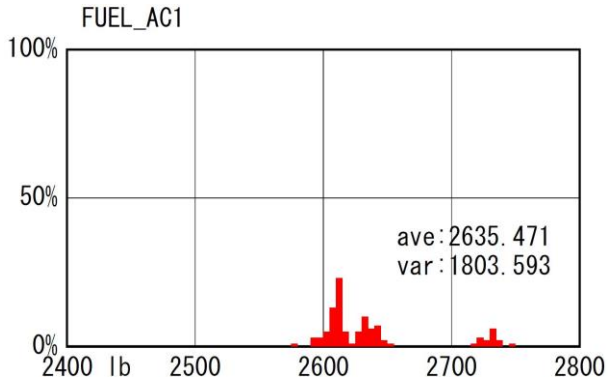

Figure 22 Fuel consumption of B777-200: 2nd aircraft

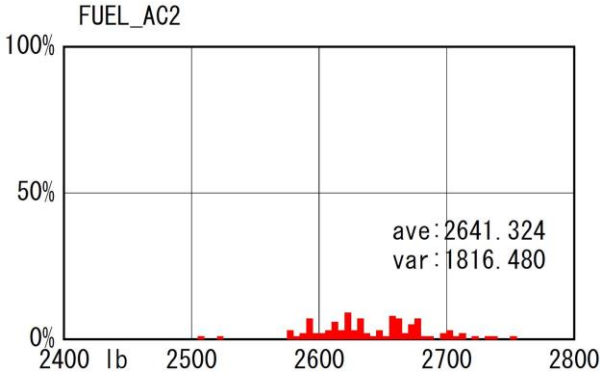

Figure 23 Fuel consumption of B777-200: 3rd aircraft

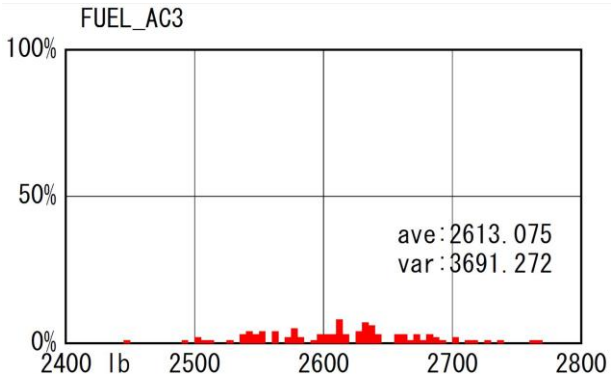

Figure 24 Fuel consumption of B777-200: 4th aircraft

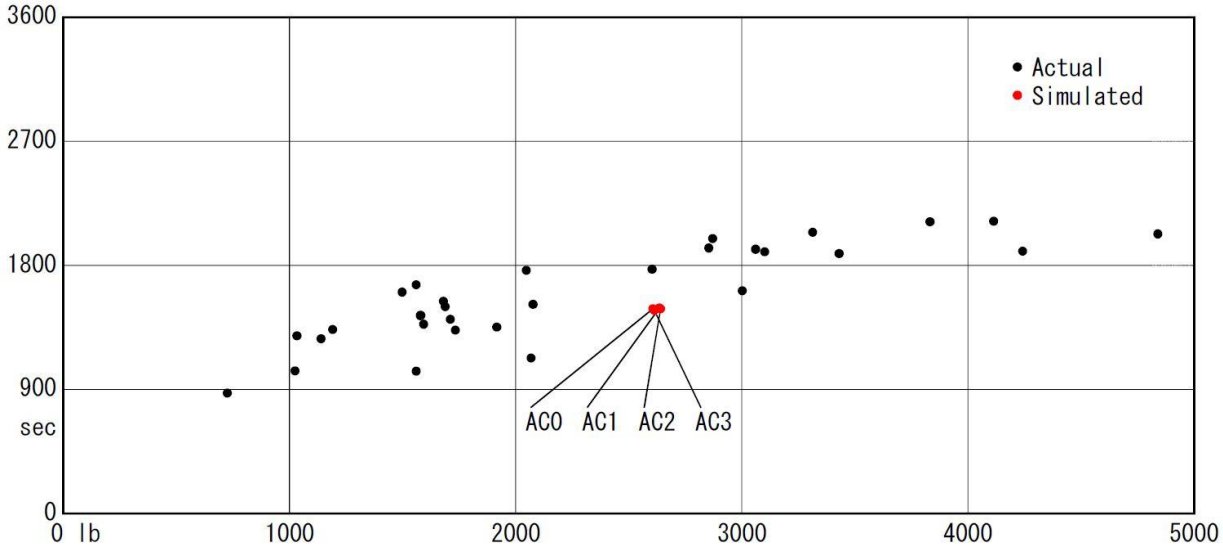

Figure 25 Comparison of fuel consumption from TOD between Case C simulations and actual B777-200 data: *AC0, AC1, AC2, and AC3 are simulated data correspond to the first, second, third, and forth aircraft in a string.*

data with the average values of the simulated data for each four aircraft: the *x*-axis shows the fuel consumption (lb), and the *y*-axis shows the required time (seconds). The figure indicates two things: (1) In the simulations, FIM-based CDO could realize an ideal descent to reduce fuel consumption even though aircraft followed a fixed 4D trajectory by controlling thrust to achieve the assigned time spacing. The air routes in the FIM application are designed to be applicable to all types of aircraft conducting FIM operations, so they do not provide an optimal route for each type. However, simulation results confirm that FIM-based CDO achieves energy saving arrivals close to the ideal descent. (2) The variances of average fuel consumption and required time from TOD for each of the four aircraft in the simulated data are significantly smaller than the variances in actual data. This indicates that applying FIM-based CDO has a potential to achieve assigned time spacing while reducing fuel consumption for all traffic, not just for specific aircraft.

Table 2 compares averages and variances of required time and fuel consumption between actual data and simulations in Fig. 25. The averages of fuel consumption in actual data are smaller than in simulated data. One reason is that because current continuous descents realize optimal flights for individual aircraft, not for the arrival traffic flow as a whole, fuel consumption is minimized for each aircraft. On the other hand, FIM-based CDO builds fixed 4D trajectories applicable to all aircraft conducting FIM operations. This idea minimizes the variances of both required time and fuel consumption as shown in Fig. 25 and Table 2. Comparing variances, the simulated data show that FIM-based CDO works to reduce the error in the required time and to reduce fuel consumption considering the whole arrival traffic flow.

TABLE2. AVERAGE/VARIANCE VALUES OF REQUIRED TIME AND FUEL CONSUMPTION BETWEEN ACTUAL AND SIMULATED DATA

		Actual data	Simulated data
Required time	Average(seconds)	1584.000	1483.904
	Variance	114738.129	75.10841
Fuel consumption	Average (lb)	2279.808	2624.258
	Variance	1093163.534	925.7471

V. CONCLUDING REMARKS

This paper applied FIM, which is one of the ASAS applications, to CDO at Tokyo International Airport in a fast-time simulation, and estimated the effectiveness of operations from the perspectives of time spacing performance and fuel consumption. The FIM application with a medium-fidelity aircraft model including VNAV and LNAV autopilot modes, an engine system, and TECS, was implemented in a fast-time simulation. Wind estimation errors were considered in the simulation assumptions. Monte Carlo simulation runs were used to evaluate the time spacing performance at the runway threshold. Arrival routes were proposed to realize FIM-based CDO at Tokyo International Airport: one removes the current altitude restriction at the terminal gate, the others are ideal shortcuts to the airport. Five cases were simulated using combinations of the designed air routes and different aircraft types. We also considered air routes that include a traffic merging point. Simulation results showed that the FIM application could reduce initial time spacing errors between a leading aircraft while conducting CDO. Fuel consumptions were estimated using engine model parameters. With validation by actual fuel consumption and required time of arrival data, the simulation results confirm that FIM-based CDO has potential to achieve assigned time spacing while achieving fuel savings for arrival traffic as a whole, not just for individual aircraft. In order to achieve even better time-

spacing performance, minimizing wind estimation errors were suggested as one of the key issues.

Our future works will analyze safety in FIM-based CDO operations and evaluate its effectiveness in both nominal and non-nominal situations. The impacts of non-nominal events, for example ADS-B failure, degraded hardware/software performance and human errors in the operational processes should be considered before introducing FIM-based CDO in the future. Since what is called an accident is a sequence of non-nominal events, safety analysis should evaluate the potential to make a critical sequence of these rare events. It will also be necessary to consider mixed equipage, the situation where some aircraft are FIM-capable and some are not, before evaluating the fully-equipped stage. We will also include more aircraft types in future simulations. Wind effects and estimation errors could be critical in speed control. Real-time simulations should be conducted to analyze hazards in pilot and ATCo behaviors before building their models in fast-time simulations. Operational issues in human factors, such as the potential for confusion between controllers and pilots in high workload situations, need to be investigated via real-time human-in-the-loop simulation studies different to this fast-time study. By collaborating with concept builders and experts on real-time simulation, our approach will be further developed to evaluate the future FIM application

ACKNOWLEDGMENT

We are grateful to Dr. Bryan Barmore and Mr. Terence Abbott of the NASA Langley Research Center and Mr. Frank Bussink of the National Aerospace Laboratory NLR for their great support on learning the ASTAR algorithm, and to Mr. Peter van der Geest of NLR for his generous tutorials on aircraft dynamics and flight control systems.

REFERENCES

[1] Study Group for the future Air Traffic Systems (MLITT) , CARATS Long-term Vision for the Future Air Traffic Systems, 2010.

[2] Federal Aviation Administration, FAA's NextGen Implementation Plan, 2011.

[3] SESAR Joint undertaking, European Air Traffic Management Mater Plan, 1st ed., 2009.

[4] RTCA, "Safety, Performance and Interoperability Requirements Document for Airborne Spacing – Flight Deck Interval Management (ASPA-FIM)", RTCA DO-328, June 22, 2011.

[5] FAA/EUROCONTROL Cooperative R&D: Action Plan 1, Principles of Operation for the Use of Airborne Separation Assurance Systems, 2001.

[6] CARE/ASAS Action, CARE/ASAS Activity 5 Description of a first package of GS/AS applications version 2.2, 2002.

[7] Itoh, E., Everdij, M., Bakker, G.J., and Blom, H., "Speed Control for Airborne Separation Assistance in Continuous Descent Arrivals", Proc. 9th American Institute of Aeronautics and Astronautics - Aviation Technology, Integration, and Operations (AIAA ATIO), 2009.

[8] Itoh, E., Everdij, M., Bakker, G.J., and Blom, H., "Speed Control for Airborne Separation Assistance in Continuous Descent Arrivals", R&D report published by National Aerospace Laboratory NLR Air Transport Safety Institute, NLR-TP-2010-328, September 2010.

[9] Itoh, E., Everdij, M., Bakker, G.J., and Blom, H., "The Impacts of Surveillance Failure on Airborne Separation Assistance System Based Continuous Descent Approach", Proc. 27th International Council of the Aeronautical Science (ICAS2010), 2010.

[10] Itoh, E., Everdij, M., Bakker, G.J., and Blom H., "Effects of Surveillance Failure on Airborne-based Continuous Descent Approach", Journal of Aerospace Engineering, Vol. 226 (ISSN 0954-4100), pp. 1470-1480, 2012.

[11] Itoh, E., Uejima, K., Chida, H., Nishinari, K., Everdij, M., Bakker, G. J., and Blom, H., "An Overview of Airborne Time-Spacing Research in the JADE Program", Proc. 2nd International Conference on Application and Theory of Automation in Command and Control Systems (ATACCS 2012), May 2012.

[12] Itoh, E., Uejima, K., Everdij, M., Bakker, G. J., and Blom, H., "Analyzing Separation Loss Events in Two-paired Aircraft Trailing Conducting Airborne Time Spacing Based Continuous Descent Arrival", Proc. 28th International Council of the Aeronautical Science (ICAS2012), 2012.

[13] Abbott, T. "A Brief History of Airborne Self-Spacing Concepts", NASA/CR-2009-215695, 2009.

[14] Abbott, T., "A Trajectory Algorithm to Support En Route and Terminal Area Self-Spacing Concepts", NASA/CR-2007-214899, 2007.

[15] Abbott, T., "An Overview of a Trajectory-based Solution for En Route and Terminal Area Self-Spacing to Include Parallel Runway Operations", NASA/CR-2011-217194, 2011.

[16] van der Geest, P., "The AMAAI Modeling Toolset for The Analysis of In-trail Following Dynamics, Deliverable D2: Description and User Guide", NLR-CR-2002-112, 2002.

[17] Everdij, M.H.C. and Blom, H.A.P., "Piecewise Deterministic Markov Processes Represented by Dynamically Coloured Petri Nets", Stochastics, Vol. 77, 2005, pp. 1–29, 2005.

[18] Everdij M.H.C. and Blom, H.A.P., "Hybrid Petri Nets with Diffusion that Have into Mappings with Generalised Stochastic Hybrid Processes", Eds: H.A.P. Blom and J. Lygeros. Stochastic Hybrid Systems: Theory and Safety Critical Applications, LNCIS series, Springer, Berlin, 2006, pp 31–64.

[19] Everdij, M.H.C., Klompstra, M.B., Blom, H.A.P., Klein Obbink, B., "Compositional Specification of a Multi-agent System by Stochastically and Dynamically Coloured Petri Nets", Eds: H.A.P. Blom, J. Lygeros. Stochastic Hybrid Systems: Theory and Safety Critical Applications, LNCIS series, Springer, Berlin, July 2006, pp. 325–350.

[20] Everdij, M.H.C. and Blom , H.A.P., "Hybrid State Petri Nets which Have the Analysis Power of Stochastic Hybrid Systems and the Formal Verification Power of Automata", Ed: P. Pawlewski, Petri Nets, Chapter 12, I-Tech Education and Publishing, Vienna, 2010, pp. 227-252.

[21] Itoh, E., Uejima, K., Kakichi, Y., and Suziki., S., "Evaluation on Airborne-based Energy Saving Arrivals to Tokyo International Airport using Modeling Approach", Proc. 2013 AIAA Guidance, Navigation, and Control (submitted in 2013).

[22] Kageyama, K., "A Basic Study on Efficiency in Japanese Airspace", Proc. 28th International Council of the Aeronautical Science (ICAS2012), 2012.

AUTHOR BIOGRAPHY

Eri Itoh received a PhD from the Department of Aeronautics and Astronautics, The University of Tokyo, Tokyo, Japan, in 2008. She worked at Eurocontrol Experimental Centre (EEC), in Brétigny-sur-Orge, France, as a doctoral researcher in October 2007- March 2008. She started to work at Air traffic Management Department in Electronic Navigation Research Institute (ENRI) , Tokyo, Japan, in 2008, and currently holds the position of senior researcher. She has been conducting research collaboration with the National Aerospace Laboratory NLR in the Netherlands since 2008.She has been a member of the program committee of the International Council of Aeronautical Science (ICAS) since 2010, and a visiting fellow with The University of Tokyo since 2012.

Kazuhiko Uejima entered The Ministry of Land, Infrastructure, Transport, and Tourism (MLITT) in Tokyo, Japan, in 1963, and contributed to the development of information processing technology of FDP, RDP, and ARTS in the Japanese ATM system. After a 32-year career as a systems engineer in Japanese ATM field, he joined NEC Corporation, Tokyo, Japan, in 1996 and worked as a senior programmer for 10 years. He currently holds a position as a simulation specialist with ENRI.